Clays and Clay Minerals, Vol. 52, No. 2, 227–239, 2004.

ULTRAMAFIC-ROCK-HOSTED VEIN SEPIOLITE OCCURRENCES IN THE ANKARA OPHIOLITIC MÉLANGE, CENTRAL ANATOLIA, TURKEY

HÜSEYIN YALÇIN AND ÖMER BOZKAYA

Cumhuriyet University, Department of Geological Engineering, TR-58140 Sivas, Turkey

Abstract—A 2 m thick brecciated zone containing magnesian minerals is present at the contact of tectonites and cumulates. Tectonites below this zone comprise serpentinized orthopyroxenite and serpentinite. An alteration zone with vein-type bedding comprises four different levels; from bottom to top they are: (1) green-brown serpentinite with dolomite (0.9 m), (2) light greenish-white dolomite with serpentine (0.5 m), (3) white dolomite with sepiolite (0.4 m), and (4) greenish-white dolomite with smectite-chlorite (0.2 m). The first level has a mineral association of serpentine + dolomite ± calcite ± aragonite, the second level consists of dolomite + serpentine ± calcite or dolomite + magnesite + serpentine, the third level comprises dolomite + sepiolite, and the fourth level is made up of dolomite + chlorite + smectite + serpentine. Dolomite, the main mineral of the alteration zone, occurs as coarse crystals (microsparitic-sparitic) in fractures and as small crystals (microsparitic-micritic) in the matrix, which includes serpentine and gabbro relics. Sepiolite developed at the edges and surfaces of dolomite and as fibrous forms in voids. Cumulate rocks above this zone comprise uralitic gabbros. The occurrences of magnesian minerals developed in three stages: the first stage was the serpentinization of olivine; the second stage was the dissolution of serpentine by groundwater and/or meteoric water containing carbon dioxide; and the last stage was the synthesis of neoformed minerals.

Key Words—Dolomite, Elmadağ, Ophicarbonate, Sepiolite, Turkey, Ultramafic.

INTRODUCTION

In a classic ophiolite sequence, the following lithologies are present in ascending order: ultramafic rocks with different proportions of serpentinized rocks and tectonite fabrics, magmatic-textured gabbroids with mylonitic fabrics, a mafic sheeted-dike complex, mafic volcanites with pillow-structured lavas, and an overlying sedimentary cover (Coleman, 1977).

The presence of carbonate minerals in peridotites of ophiolite sequences indicate that CO_2 metasomatism or carbonatization (and the addition of CO_2) occurs at 200–300ºC (Schandl and Wicks, 1993). The serpentinites consist mainly of serpentine minerals, and in some cases magnetite, brucite and Mg- and Ca-Al-silicates. Carbonate minerals are replaced in serpentinite rather than in peridotite, and the mineral assemblages formed by low-temperature carbonatization consist of talc + carbonate or quartz + carbonate, and include serpentine relics (Abu-Jaber and Kimberley, 1992; Peabody and Einaudi, 1992; Lambert and Epstein, 1992).

Sepiolite occurs abundantly in Tertiary rocks, especially those rich in phosphates, salt, sulfates, carbonates and zeolites, and also in siliceous rocks, and in various environments such as pedogenic, lacustrine, lagoonal and marine (Singer and Galán, 1984). Nodular and layered sepiolites are present in some Neogene lacustrine basins (Yeniyol, 1986, 1992, 1993; Ece and Çoban, 1994; Yalçın and Bozkaya, 1995a; Ece, 1998) and in some Paleocene marine sediments (Yalçın and Bozkaya, 1995b).

The Elmadağ ophicarbonates, located between serpentinized ultramafic rocks and gabbroids, are quite different from those mentioned in the literature (Singer and Galán, 1984). In this study, we consider in detail the environment and mechanism of formation (weathering) of these rocks, and their mineralogical features such as the fact that they contain sepiolite instead of brucite, talc and quartz.

GEOLOGICAL SETTING AND STRATIGRAPHY

The present-day geology of Anatolia has been dominated by the convergence of the African and Arabian plates with Eurasia, leading to the closure of the northern branch of Neotethys (Şengör and Yılmaz, 1981). It is generally believed that the northern Neotethyan Ocean began to close in the Late Cretaceous, and that collision and amalgamation of continental fragments began in the Middle Eocene; these fragments took on their present disposition in the Middle Miocene. N–S shortening and thickening across Anatolia continues today. The collision was accompanied by obduction of the Tethyan oceanic crust towards and onto the neighboring continental terranes that resulted in the development of the Ankara ophiolitic mélange. The Ankara Mélange, first named by Bailey and McCallien (1950), is located between the Pontide Belt to the north, the Tauride Belt to the south, and the Central Anatolian Crystalline Complex to the east. This unit is composed mainly of imbricated sedimentary mélange with meta-

* E-mail address of corresponding author:
yalcin@cumhuriyet.edu .tr
DOI: 10.1346/CCMN.2004.0520209

morphosed limestone slices of Permian-Triassic age and tectonic mélange with ophiolitic slices of Late Cretaceous age (Çapan *et al.*, 1983). Sepiolite occurrences are restricted to the ophiolitic mélange. The emplacement of ophiolites in the Pontides is assumed to be Middle Eocene in age (Yılmaz *et al.*, 1997). Therefore, the age of these sepiolite occurrences may possibly be younger than Eocene, perhaps Middle Miocene related to a new tectonic event (*e.g.* Şengör, 1979).

In this study, a geological map prepared by Çelik (1989) was used, although a number of investigations have been carried out on the general geology of the district (Figure 1). The stratigraphic sequence is summarized as follows: The oldest unit in the region is the Kusunlar formation of Carboniferous–Lower Triassic age consisting of metasandstone-slate alternations. In the study area, the Upper Triassic-Lias Elmadağ complex includes matrix constituents such as graywacke, subgraywacke-claystone and volcanic rocks and blocks of limestone and dikes and lava flows having spilitic basaltic, basaltic and dioritic compositions and different ages (Carboniferous, Permian and Triassic). The Upper Cretaceous Kılıçlar complex is subdivided into four members, namely the Edige serpentinite that hosts the sepiolite occurrences, the Çanakçıtepe limestone, the Akkesmetepe limestone, and the Ilıcapınar radiolarite. These units are represented by Triassic and Upper Jurassic–Lower Cretaceous rocks, such as limestone blocks, diabase, diorite, basalt, spilitic basaltic dykes, and lava flows, and generally by serpentinized ultramafic rocks in a matrix of sandstone-claystone and volcanic rocks. The Kayaş formation is composed of volcanic rocks, tuff-tuffite and lacustrine limestone, and occurs throughout most of the study area.

LITHOLOGY

A 2 m thick zone of magnesian minerals parallels the main thrust fault, situated approximately N45ºE, 45ºSE between the tectonites and cumulate rocks of the ophiolitic series (Figure 2). The tectonites in the lower part of this zone comprise typically fractured, green-black serpentinized olivine-orthopyroxenites and mesh-structured, green serpentinite breccias. Four different levels, which pass irregularly into one another, comprise the ophicarbonate (serpentine-carbonate rock; O'Hanley, 1996) zone with its vein-type bedding. The first level is characterized by a 0.9 m thick green-brown serpentinite. The second level is a 0.5 m thick light greenish-white dolomite with serpentinite. The third level is 0.4 m thick and contains partly brecciated, tough white dolomite with sepiolite. The uppermost level has a thickness of 0.2 m and comprises greenish-white dolomite with chlorite. The second and third levels are possibly lateral

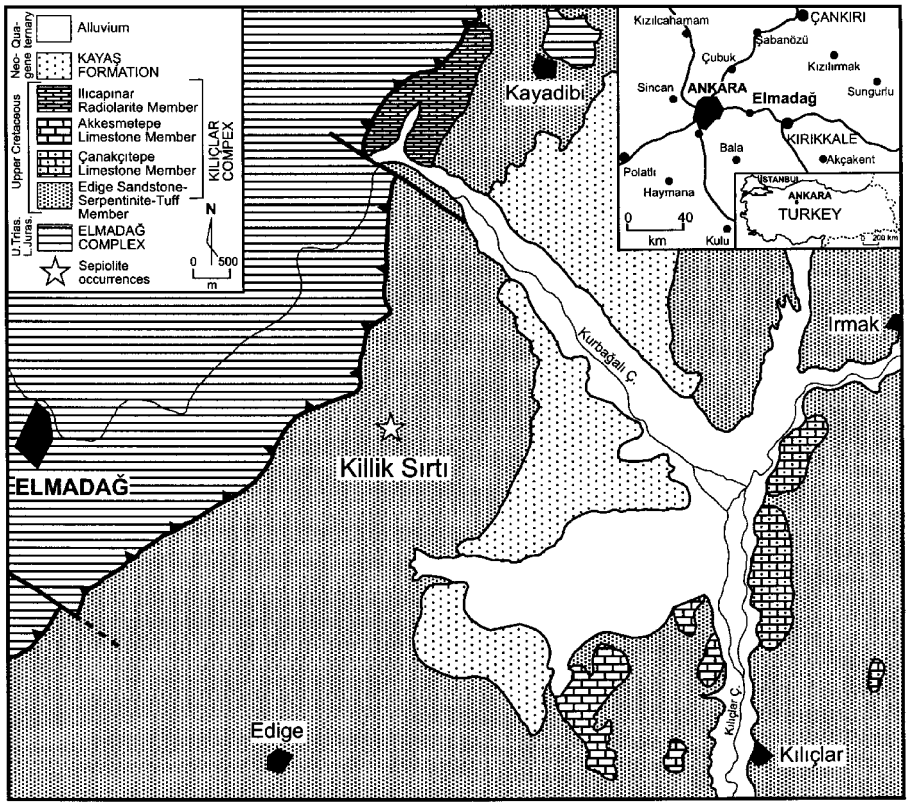

Figure 1. Location and geological map of the study area (Çelik, 1989).

https://doi.org/10.1346/CCMN.2004.0520209 Published online by Cambridge University Press

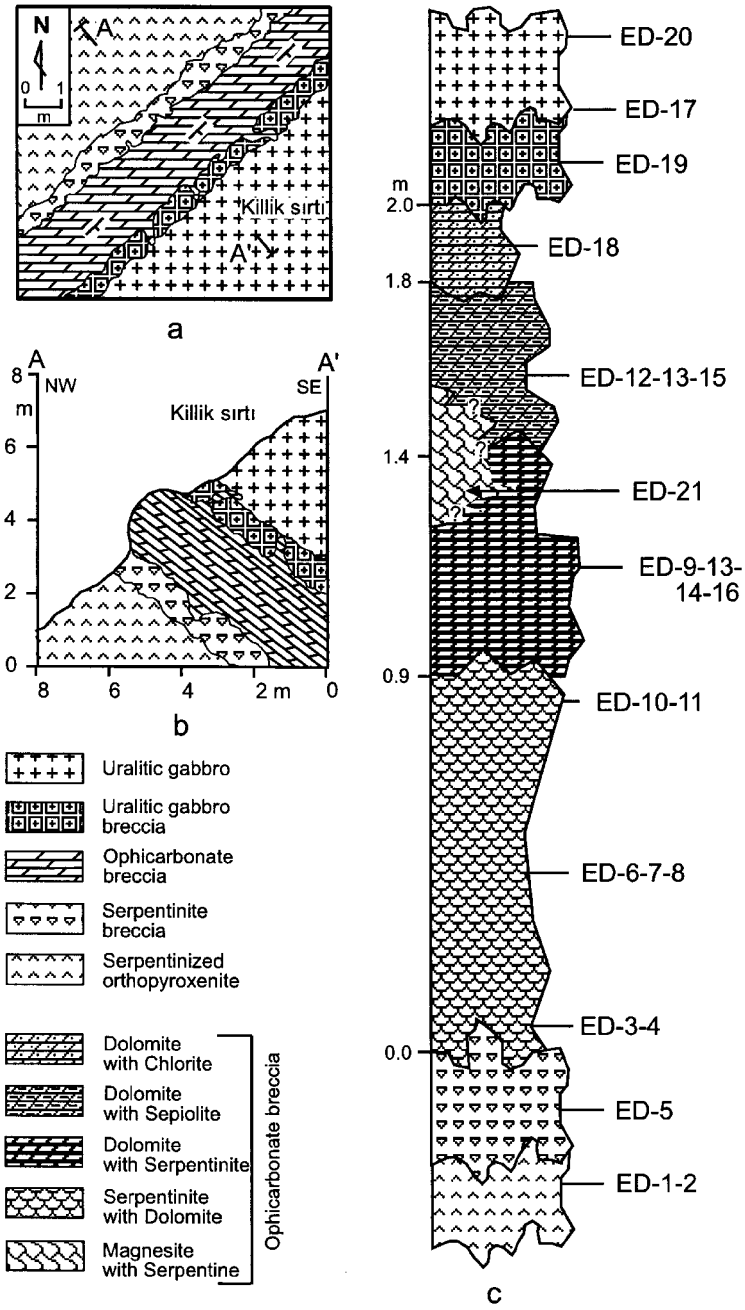

Figure 2. (a) Simplified geological map, (b) geological section, and (c) stratigraphic columnar section of ophicarbonates in the Elmadağ area.

transitions to serpentine-magnesite with dolomite. Commercial magnesite deposits in the region are hosted by serpentinites and occur as fracture fillings and masses.

MATERIAL AND METHODS

A total of 21 rock and mineral samples, taken from the carbonatized alteration zone, were examined by optical microscopy, X-ray diffractometry (XRD), X-ray fluorescence spectrometry (XRF), and differential thermal analysis-thermogravimetry (DTA-TGA) in the laboratories of Cumhuriyet University; by scanning electron microscopy (SEM) in the laboratories of Istanbul Technical University, and by inductively coupled plasma-mass spectrometry (ICP-MS) in Activation Laboratories Ltd. (Canada).

Powder XRD was performed using a Rigaku DMAX IIIC instrument with CuKα radiation at 35 kV and 15 mA and slits (divergence = 1°, scatter = 1°, receiving

https://doi.org/10.1346/CCMN.2004.0520209 Published online by Cambridge University Press

= 0.15 mm, receiving-monochromator = 0.30 mm), and with a scan speed of 2°2θ/min (oriented clays with a scan speed of 1°2θ/min, treated with ethylene glycol and left in a desiccator at 60ºC for 16 h and then heated to 490ºC for 4 h). The semi-quantitative percentages of rock-forming minerals were calculated using the external standard method of Brindley (1980). The sedimentation method, following complete carbonate removal with HCl, was used for clay/phyllosilicate separation. Diffraction data records of 001 basal reflections of clay minerals were evaluated according to the intensity factors of Moore and Reynolds (1997). The 211 peak of quartz at 59.982°2θ, d = 1.541 Å was used as an internal standard for measurements of the d spacings of clay minerals.

High-temperature treatments of phyllosilicate minerals were conducted on a Shimadzu DT-TG-50 coupled thermal analyzer. Al_2O_3 reference material and 10 mg sample powders were placed in platinum pans and heated to 1050ºC in air at a rate of 10ºC/min. Paper speed and interval were adjusted as 4 mm/min and ±100 mV, respectively.

Chemical compositions of serpentine and sepiolite were quantified using a Rigaku 3270 XRF instrument calibrated against USGS (Flanagan, 1976), CRPG, GIT-IWG and ANRT (Govindaraju, 1989) international rock standards to check the reliability of the results. The analytical reproducibility of this method was ±2% for the major elements, and ±5% for some trace elements. Trace and rare-earth element contents of a sepiolite sample (ED-12) were measured by ICP-MS. The content of water and other volatiles (*i.e.* loss on ignition, LOI, in wt.%), was determined by drying the samples at 110ºC for 16 h, then by heating to 1000ºC and weighing the samples; the differences between the before and after sample weights are the LOIs of the samples.

OPTICAL MICROSCOPY

Three types of serpentinite texture have been recognized on the basis of the extent of preservation of the protolith texture: these are pseudomorphic, non-pseudomorphic and transitional textures (Wicks and Whittaker, 1977; Wicks and Plant, 1979). Of these, pseudomorphic texture is represented in the study area by widespread mesh texture developed in serpentinized olivines. The peridotites consist mainly of enstatite and olivine and, in some cases, chromite.

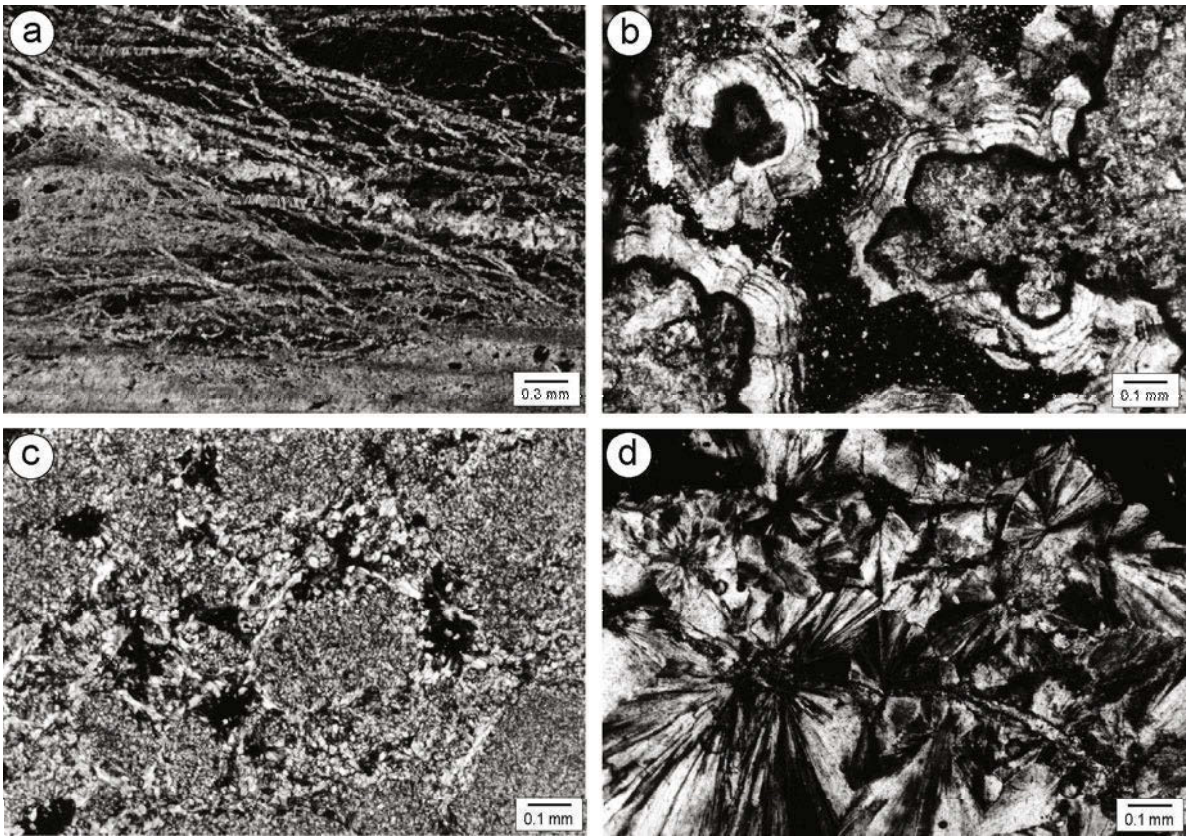

Figure 3. Optical microscopy images, (a) microsparitic dolomite crystals developed within the cracks of serpentinite with dolomite (ED-6, crossed nicol = cn), (b) gel-textured dolomites (ED-11, cn), (c) fibrous sepiolites developed within pores and surroundings of sparitic dolomites (ED-12, cn), (d) rod and radial anthophyllite minerals developed within the cracks of uralitic gabbros (ED-19, cn).

https://doi.org/10.1346/CCMN.2004.0520209 Published online by Cambridge University Press

The serpentinized enstatites with bastite texture include clinopyroxene lamellae and lizardite ribbons within fractures. Olivine relics have not been observed in the serpentinites although mesh texture is typically preserved. These textural observations suggest that the serpentinites were derived from dunites.

Microsparitic dolomite crystals fill fractures in the serpentine matrix of the serpentinite, with dolomite in the first level of the ophicarbonates (Figure 3a). The serpentine minerals have fibrous/acicular form and in places constitute ribbons. In a thin-section of another sample, nodular serpentines are surrounded by dolomites and, in another sample, dolomites have a gel texture (Figure 3b). In the dolomites (with serpentine) of the second level, platy serpentine minerals and chloritized and/or serpentinized mafic-ultramafic fragments are found within the carbonate cement. In the dolomites (with sepiolite) of the third level, fibrous sepiolite is present in voids and surrounding sparitic dolomites (Figure 3c). Dolomites (with chlorite) of the fourth level commonly include chloritized mafic-ultramafic rock fragments within the carbonate cement.

Gabbros in the uppermost level contain typically uralitized (hornblende and tremolite/actinolite) and partly serpentinized and chloritized pyroxene, and argillaceous/ sericitized plagioclase, as well as accessory minerals such as epidote and titanite. Rod-shaped and radial anthophyllite that developed along a fracture were encountered in one sample (ED-19).

SCANNING ELECTRON MICROSCOPY

Fibrous clay minerals are clearly visible in all photomicrographs. Dolomite with sepiolite highlights the mesh texture of the original serpentinite (Figure 4a). The size of the globular-ellipsoidal meshes that replace serpentine minerals ranges from ~5 to 100 μm, but is generally 10–25 μm. The fiber bunches of sepiolite develop from the edges of and voids in dolomite and surround them, thus indicating that these minerals may very well have developed together (Figure 4b). Sepiolite fibers have also grown on the surfaces of dolomites (Figure 4c). The lengths and thicknesses of bent sepiolite fibers range 1–20 μm and 0.1–0.3 μm, respec-

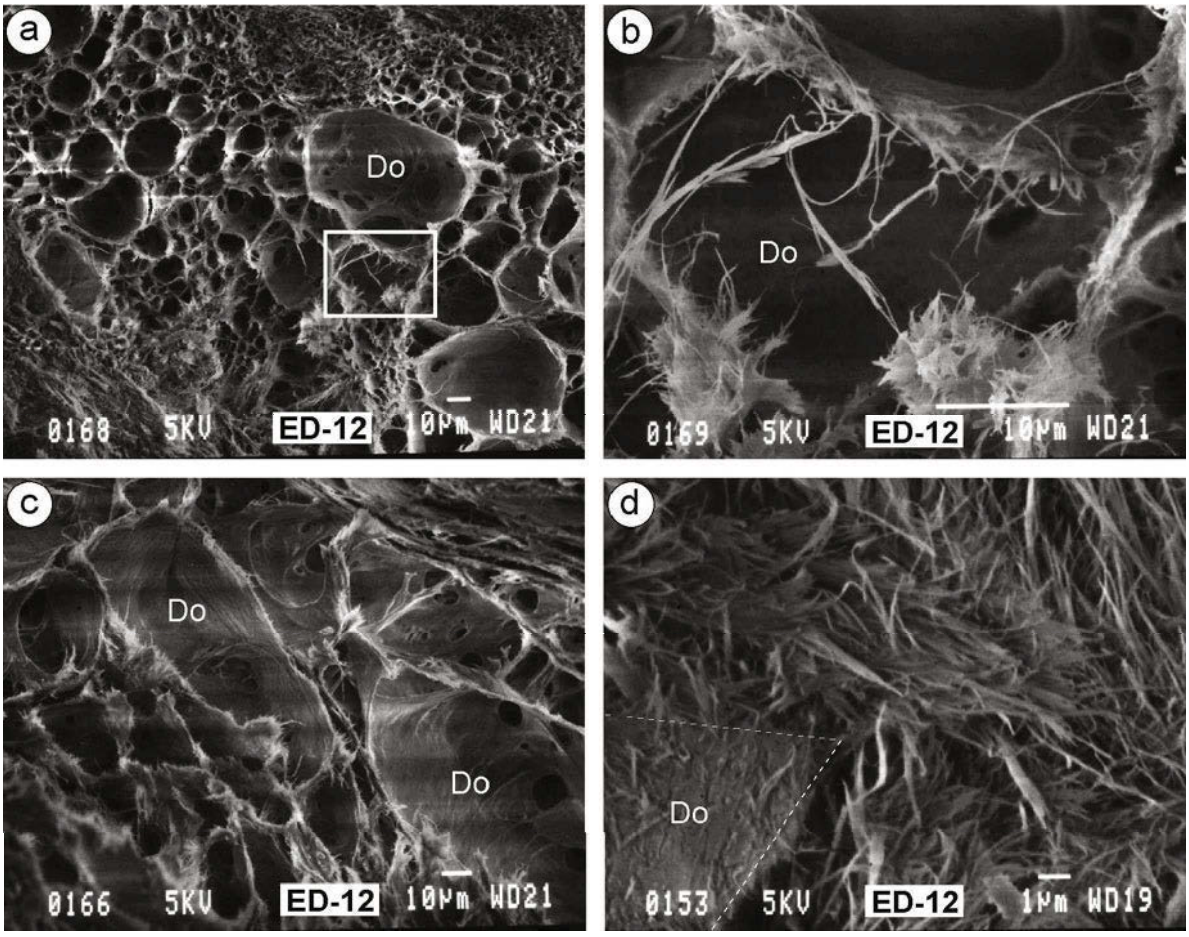

Figure 4. SEM images of sepiolite and dolomite (Do): (a) the mesh texture in the dolomites with sepiolite; (b) sepiolite bunches developed on the edges of dolomites; (c) sepiolite fibers on the surface of dolomites; (d) sepiolite fibers and bunches formed on the surface and edges of nearly rhombohedral dolomites.

https://doi.org/10.1346/CCMN.2004.0520209 Published online by Cambridge University Press

tively. Sepiolite fibers are visible on the surfaces of dolomites (with partly rhombohedral-like morphology in the left corner of the other photomicrograph, Figure 4d). These textural relationships agree with the work of Yalçın and Bozkaya (1995b).

X-RAY DIFFRACTOMETRY

According to powder XRD results, serpentine is the only rock-forming mineral in the serpentinite breccia at the base of the ophicarbonate alteration zone. The main minerals of the first level are serpentine and dolomite accompanied by trace amounts of calcite, and scarce aragonite in one sample.

The amount of dolomite increases in the second level and, in order of abundance, serpentine, sepiolite, smectite and chlorite are the predominant phyllosilicate minerals that occur. The third and fourth levels contain the mineral associations dolomite + sepiolite and dolomite + chlorite + smectite, respectively. Phyllosilicates are represented entirely by chlorite in two samples and by chlorite + serpentine in one sample from the uralitic gabbros.

In the altered rocks, serpentine minerals constitute between ~25 and 80% of the ophidolomites but are not present in the dolomites with sepiolite.

X-ray diffraction patterns of oriented samples of the phyllosilicate minerals are given in Figure 5. Serpentines, which predominate in the first level, are easily distinguishable from chlorites by means of their 002 reflections (Figure 5a). In particular, an important intensity loss in the heated pattern and swelling (0.20 Å) in the glycolated pattern are recognized in the 110 peaks of the sepiolites (Figure 5b). Smectites are minerals characterized by expansion of 001 peaks after ethylene-glycol treatment and their reduction by heating treatment (Figure 5c,d). The 004 reflections of chlorites shift slightly to the right ($\Delta 2\theta$ = 0.31°, 0.044 Å) in the heated pattern, accompanied by a decrease in intensity (Figure 5d).

X-ray diffraction patterns of unoriented samples of the Elmadağ sepiolites indicate that they are similar to those of Hekimhan (Yalçın and Bozkaya, 1995b), but differ from those of Eskişehir with their sharper and higher-intensity peaks, and their crystallinity (Figure 6). The polytypes of the serpentine-subgroup minerals are identified by using distinctive reflections in the XRD pattern of unoriented samples. Based on the method of Bailey (1988), these minerals have polytypes of the C-structural group, with greater intensity of peaks at 2.498, 2.147 and 1.789 Å; however, there is a layered triclinic (1*T*) one discernible via the presence of peaks at 3.85 and 4.59 Å.

DIFFERENTIAL THERMAL ANALYSES

The DTA curves of sepiolite (Figure 7a) can be evaluated by separating three regions as palygorskite

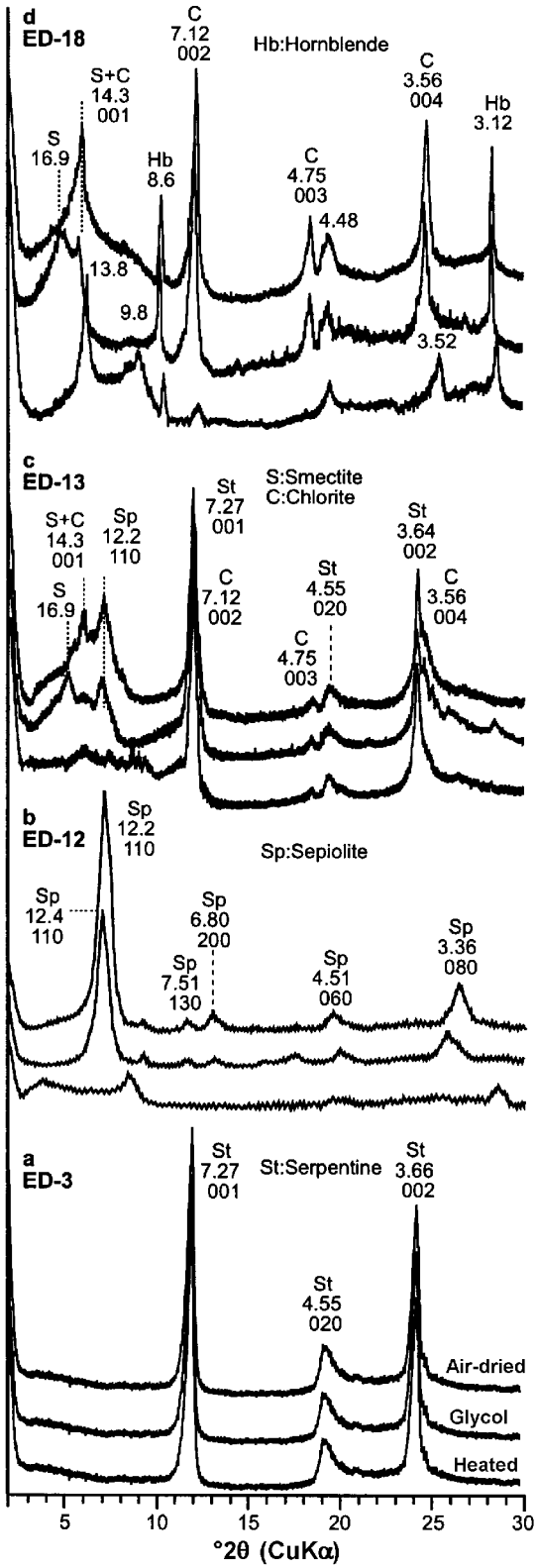

Figure 5. XRD patterns of oriented phyllosilicate minerals, (a) serpentine, (b) sepiolite, (c) serpentine + smectite + sepiolite + chlorite, (d) chlorite + smectite.

https://doi.org/10.1346/CCMN.2004.0520209 Published online by Cambridge University Press

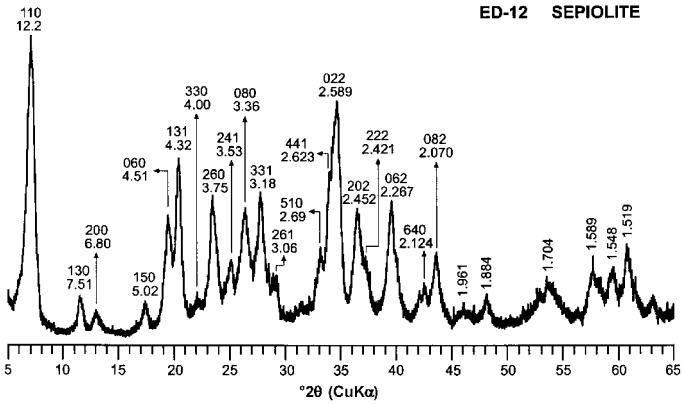

Figure 6. XRD patterns of unoriented powder sepiolite.

(Jones and Galán, 1988). Two endothermic peaks are present in the low-temperature field (<300ºC); the first is large and sharp at 72ºC between 18 and 106ºC, and the second is smaller at 275ºC between 238 and 312ºC, corresponding to the loss of adsorbed and zeolitic (hydration) water, respectively. The second endothermic peak at 526ºC is broad, from 424 to 619ºC, and exists in the central field (300–750ºC). The final endothermic peak at 810ºC, expanding from 760 to 848ºC, is in the high-temperature field (>750ºC). These endothermic variations show retention of bound (coordination – OH_2) and crystallization (dehydroxylation – OH) water within the structure. An exothermic peak at 864ºC is sharp, beginning at 843ºC and ending at 864ºC. The crystal structure of sepiolite has collapsed, and a new mineral with a similar chemistry (enstatite) formed in this last reaction. The exothermic peak of palygorskite appears at a temperature of >1000ºC, compared to the high-temperature behavior of sepiolite-palygorskite-group minerals (Yalçın and Bozkaya, 1995a).

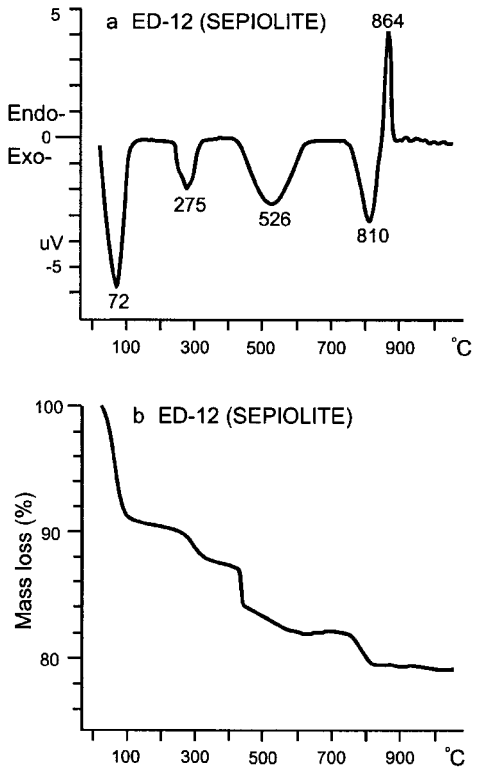

Figure 7. High-temperatures curves of sepiolite, (a) DTA, (b) TGA.

Three dehydration steps and five dehydroxylation steps are observed in the TGA curve of sepiolite (Figure 7b), as proposed by Frost and Ding (2003), demonstrating that both bound and crystallization water are lost more rapidly and over shorter temperature intervals than zeolitic water. A total mass loss of 20% consisted of 8% adsorbed, 5% zeolitic, 4% bound and 3% crystal waters. In other words, the total weight loss of sepiolite is 12%, excepting adsorbed water, and there is reasonable agreement between measured (LOI) and theoretical values.

GEOCHEMISTRY

The major- and trace-element contents of some rock and serpentine samples are given in Table 1. The structural formulae of sepiolites, calculated on the basis of 32 oxygen atoms (Weaver and Pollard, 1973), along with average values of well known sepiolites of Turkey, are presented in Table 2. Some trace- and rare-earth element contents of the Elmadağ sepiolites are also displayed in Table 3.

The major chemical constituents of the host rock and rock-forming silicate minerals are exhibited in the SiO_2-(Al_2O_3+ΣFe_2O_3)-MgO triangular diagram (Figure 8a). Samples are stacked, and are divided into two groups, namely serpentinized peridotite + serpentinites and sepiolites. These stackings are also clear in the SiO_2-CaO-MgO triangular diagram, in which mineral phases are added on the basis of mineral assemblages (Figure 8b). Sepiolite, serpentine and magnesite, and carbonates are arranged along the SiO_2-MgO and CaO-MgO lines, respectively. These variations reveal that the

https://doi.org/10.1346/CCMN.2004.0520209 Published online by Cambridge University Press

Table 1. Major (wt.%) and trace (ppm) element analyses of some rocks and minerals related to ultramafics from the Elmadağ area, Central Anatolia.

Rock/mineral	Serpentinized olivine-orthopyroxenite		Serpentinite	Serpentine	
Sample	ED-1	ED-2	ED-5	ED-3	ED-10
SiO_2	38.49	39.48	33.68	41.97	43.82
TiO_2	0.00	0.00	0.00	0.00	0.00
Al_2O_3	1.50	1.54	1.19	1.25	1.47
ΣFe_2O_3	11.20	9.69	10.08	7.28	3.66
MnO	0.18	0.18	0.13	0.15	0.04
Cr_2O_3	0.48	0.60	0.23	0.14	0.11
NiO	0.48	0.38	0.64	0.47	0.16
MgO	35.60	37.22	40.77	36.92	40.49
CaO	0.87	1.11	0.45	0.42	0.25
Na_2O	0.00	0.00	0.00	0.02	0.01
K_2O	0.00	0.00	0.00	0.00	0.00
P_2O_5	0.03	0.02	0.02	0.03	0.03
LOI	10.83	10.18	13.09	12.08	10.30
Total	99.66	100.40	100.28	100.73	100.34
Cr	3252	4086	1589	991	745
Ni	3692	3022	4998	3704	1268
Co	39	34	35	25	12
Cu	38	4	5	8	12
Pb	4	1	4	12	21
Zn	63	66	71	61	63
Rb	17	17	16	17	17
Ba	3	3	4	4	7
Sr	13	11	9	38	50
Ga	5	5	5	4	4
Nb	2	2	2	2	3
Zr	6	6	5	7	8
Y	<1	<1	<1	<1	1
Th	<1	<1	<1	<1	<1

LOI: loss on ignition

serpentine minerals have compositions similar to the peridotites, and that Ca entered into the alteration environment later. The alteration trend might have been caused by serpentine to magnesite passing into the dolomite + sepiolite interphase.

The aforementioned relations can also be seen in the chondrite-normalized diagram (Taylor and McLennan, 1985) in which some minor and trace elements in the serpentine minerals, serpentinized peridotite and serpentinite are compared (Figure 9). The most remarkable feature is that sepiolite is wholly unlike the samples derived from ultramafic rocks. Sepiolite has marked positive Ba and Sr anomalies, and a negative Tl anomaly. Relative to chondrite, a 2–100× enrichment in Rb, Pb, Ba, Sr and Zr, and a 5–95× depletion of other trace and rare-earth elements are observed in the sepiolite. In spite of this, compared to chondrite, an 8–80× depletion of Cr, Ni, Cu and Zn, and enrichment in other elements are pronounced in the serpentinized peridotite + serpentinite. These data indicate that

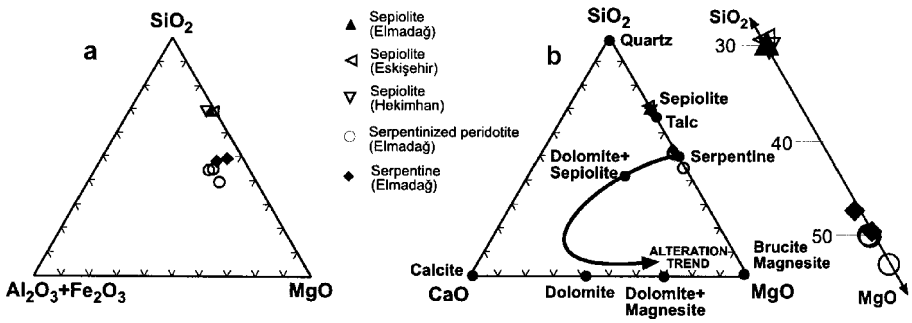

Figure 8. The compositional distributions of the Elmadağ ultramafic rocks and their alteration products on the triangular diagrams: (a) SiO_2-(Al_2O_3+Fe_2O_3)-MgO, (b) SiO_2-CaO-MgO.

https://doi.org/10.1346/CCMN.2004.0520209 Published online by Cambridge University Press

Table 2. Major element analyses (wt.%) and the unit-cell compositions of sepiolites from different deposits of Turkey.

Area	Elmadağ		Eskişehir	Hekimhan
Sample	ED-12	ED-15	ES-1	ÖB-171
SiO_2	61.83	62.14	54.13	60.30
TiO_2	0.00	0.00	0.02	0.01
Al_2O_3	1.54	1.33	0.25	0.67
ΣFe_2O_3	0.06	0.01	0.13	2.14
MnO	0.00	0.00	0.02	0.01
Cr_2O_3	0.00	0.00	0.01	0.38
NiO	0.15	0.10	0.17	0.25
MgO	26.30	26.52	23.75	24.32
CaO	0.17	0.17	0.01	0.13
Na_2O	0.00	0.00	0.03	0.04
K_2O	0.00	0.00	0.02	0.06
P_2O_5	0.02	0.02	0.02	0.06
LOI	10.38	9.88	20.33	11.07
Total	100.45	100.17	98.89	99.44
Si	11.92	11.94	11.99	11.96
Al^{IV}	0.08	0.06	0.01	0.04
Al^{VI}	0.27	0.25	0.06	0.12
Fe^{VI}	0.01	0.00	0.02	0.32
Cr	0.00	0.00	0.00	0.06
Ni	0.02	0.02	0.03	0.04
Mg	7.56	7.60	7.84	7.19
Ca	0.04	0.04	0.00	0.03
Na	0.00	0.00	0.01	0.02
K	0.00	0.00	0.01	0.02
TOC	7.86	7.86	7.95	7.73
TC	−0.08	−0.06	−0.01	−0.04
OC	−0.01	−0.03	−0.02	−0.04
TLC	−0.08	−0.03	−0.03	−0.10
ILC	0.07	0.07	0.02	0.10

LOI: loss on ignition, TOC: total octahedral cation
TC: tetrahedral charge, OC: octahedral charge
TLC: total layer charge, ILC: interlayer charge

Table 3. Trace element analyses (ppm) of sepiolites from the Elmadağ area, Central Turkey.

Sample	D-12	ED-15
Cr	29	38
Ni	511	747
Co	2	1
V	<5	n.a.
Cu	<10	17
Pb	53	50
Zn	30	48
Bi	0.27	n.a.
In	<0.1	n.a.
Sn	<1	n.a.
W	13.3	n.a.
Mo	<2	n.a.
As	<5	n.a.
Sb	<0.2	n.a.
Ge	0.8	n.a.
Ag	<0.5	n.a.
Rb	<2	17
Cs	0.1	n.a.
Ba	400	350
Sr	8	41
Tl	<0.01	n.a.
Ga	1	6
Ta	<0.1	n.a.
Nb	<0.5	3
Hf	0.1	n.a.
Zr	4	8
Y	<0.5	<1
Th	0.06	<1
U	<0.05	n.a.
La	0.11	n.a.
Ce	0.2	n.a.
Pr	0.02	n.a.
Nd	0.10	n.a.
Sm	<0.02	n.a.
Eu	<0.005	n.a.
Gd	<0.02	n.a.
Tb	<0.01	n.a.
Dy	<0.02	n.a.
Ho	<0.01	n.a.
Er	0.02	n.a.
Tm	<0.005	n.a.
Yb	0.01	n.a.
Lu	0.002	n.a.

n.a.: not analyzed

element distributions are controlled by reactions in the alteration process.

The mean chemical composition of the serpentines gives lizardite from the Mg-Al serpentines (lizardite = $Mg_3Si_2O_5(OH)_4$ and amesite = $(Mg_2Al)SiAlO_5(OH)_4$) or Fe-lizardite from the Mg-Fe serpentines (lizardite = $Mg_3Si_2O_5(OH)_4$ and cronstedtite = $(Fe_2Fe^{3+})SiFeO_5(OH)_4$), probably representing a solid-solution series on the basis of the nomenclature of Wicks and O'Hanley (1988).

Tetrahedral substitution for Al is less, but the most important substitution for Al is in the octahedral sheet. This chain-structure phyllosilicate is termed Al-sepiolite as proposed by other workers (Jones and Galán, 1988; Galán and Carretero, 1999):

$$Ca_{0.04}(Mg_{7.58}Al_{0.26}Ni_{0.02})Si_{11.93}Al_{0.07}O_{30}(OH)_4(OH_2)_4$$

The Elmadağ sepiolites are richer in Al on account of unit-cell composition as compared to the Eskişehir lacustrine and Hekimhan marine sepiolites (Yalçın and Bozkaya, 1995b). On the other hand, they are poorer in Mg, Fe and some trace elements such as Cr and Ni. Additionally, a reasonable amount of trace elements and *REE*s reveals the absence of other clay phases and/or heavy minerals in the sepiolitic fractions.

ORIGIN AND FORMATION

In the system $MgO-SiO_2-H_2O$, the low-temperature limit determined in the anthophyllite = enstatite + talc equilibrium is ~450ºC, taking into consideration low pressure (<1 kbar) and Fe differentiation (Evans and Guggenheim, 1988). Lizardites derived from olivines form at temperatures <260ºC, as shown in the equilibrium diagram of the same authors.

https://doi.org/10.1346/CCMN.2004.0520209 Published online by Cambridge University Press

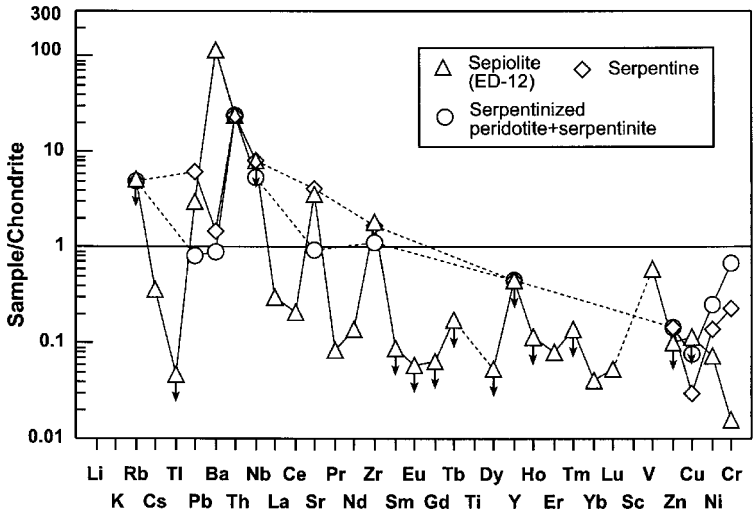

Figure 9. The multiple spider diagram of the Elmadağ ultramafic rocks and their alteration products (arrows show the values of detection limits; chondrite (Taylor and McLennan, 1985)).

Mineral associations such as olivine + enstatite + lizardite and enstatite + tremolite/actinolite + anthophyllite in the peridotites and gabbros of the Elmadağ region suggest that serpentinization of the peridotites and uralitization of the gabbros occurred at different temperatures and times, although various thermodynamic parameters – such as total pressure, water pressure, oxygen fugacity, activities of oxides, *etc.* – can cause increases or decreases in temperature.

Mineral parageneses and textural properties of the Elmadağ ophicarbonates indicate that the alteration developed at low pressures. The presence of a small amount of aragonite in a single sample does not reduce the validity of this observation. It has been found that aragonite can precipitate from seawater at low temperatures, as determined in a serpentine diapir of the Mariana forearc (Sakai *et al.*, 1991) and carbonate-altered peridotites in the near mid-ocean ridge (Bonatti *et al.*, 1974). Such occurrences indicate that aragonite which accompanies serpentinites does not prove high-pressure crystallization.

Although whether the mafic-ultramafic rocks are serpentinized during or before the emplacement of ophiolites on the continents is still debated, serpentinite-related mineralization is simply divided into three groups (Mittwede, 1996): (1) magmatic or pyrogenetic (pre-serpentinization), (2) syngenetic (directly related to the serpentinization process), (3) epigenetic (post-serpentinization, covering metamorphism, alteration and weathering). The presence of smectite and chlorite suggest that the Elmadağ ophicarbonate and sepiolites are epigenetic. The serpentinization of forsterite by the action of water is the first stage in the alteration process:

$$\underset{\text{forsterite}}{2Mg_2SiO_4} + 3H_2O \rightarrow \underset{\text{serpentine}}{Mg_3Si_2O_5(OH)_4} + Mg^{2+} + 2OH^-$$

The formation of only lizardite from among the serpentine-subgroup minerals (lizardite, antigorite, chrysotile) by the hydration of forsterite, and the absence of brucite, talc and magnetite, suggest that the following reactions probably did not attain equilibrium and suitable pressure-temperature conditions:

$$\underset{\text{forsterite}}{2Mg_2SiO_4} + 3H_2O \rightarrow \underset{\text{serpentine}}{Mg_3Si_2O_5(OH)_4} + \underset{\text{brucite}}{Mg(OH)_2}$$

$$\underset{\text{forsterite}}{6Mg_2SiO_4} + 3H_2O \rightarrow \underset{\text{serpentine}}{Mg_3Si_2O_5(OH)_4} + \underset{\text{talc}}{Mg_3Si_4O_{10}(OH)_2} + 6Mg^+$$

$$\underset{\text{fayalite}}{3(Mg,Fe)_2SiO_4} + 3H_2O \rightarrow \underset{\text{serpentine}}{Mg_3Si_2O_5(OH)_4} + \underset{\text{magnetite}}{Fe_3O_4} + 2OH^-$$

The fact that the assemblages are free of brucite, talc and quartz indicate that the following reactions have also not occurred in the Elmadağ ophicarbonates:

$$\underset{\text{serpentine}}{Mg_3Si_2O_5(OH)_4} + H_2O \rightarrow \underset{\text{brucite}}{3Mg(OH)_2} + \underset{\text{quartz}}{2SiO_2}$$

$$\underset{\text{serpentine}}{Mg_3Si_2O_5(OH)_4} + 4H_4SiO_4 \rightarrow \underset{\text{talc}}{Mg_3Si_4O_{10}(OH)_2} + \underset{\text{quartz}}{2SiO_2} + 9H_2O$$

Sepiolites are late mineral phases that develop in a weathering environment under basic conditions. In the studied samples, the evidence for neoformed morphologies as revealed in the sepiolites is well established. The dissolution of serpentine by means of meteoric and/or groundwater (containing carbon dioxide or carbonic acid) moving along thrust and shear planes during or after mélange formation is the second stage of the alteration process. The occurrences of various carbonate

https://doi.org/10.1346/CCMN.2004.0520209 Published online by Cambridge University Press

and/or sepiolite associations are the third stage of the alteration process, and are related to Mg/(Mg+Ca) (magnesite 1.00, dolomite 0.50, calcite/aragonite 0.00), H_2O/CO_2 (calcite/aragonite 4.00, dolomite 0.83, magnesite 0.67) and MgO/SiO_2 (serpentine 1.50, talc 0.75, sepiolite 0.67 and quartz 0.00) ratios. From that fact, the following equations can be deduced easily:

$$\underset{\text{serpentine}}{Mg_3Si_2O_5(OH)_4} + 5H_2O + 6CO_2 + 3Ca^{2+} \rightarrow \underset{\text{dolomite}}{3CaMg(CO_3)_2} + 2H_4SiO_4 + 6H^+$$

$$\underset{\text{serpentine}}{Mg_3Si_2O_5(OH)_4} + 6H_2O + 7CO_2 + 4Ca^{2+} \rightarrow \underset{\text{dolomite}}{3CaMg(CO_3)_2} + \underset{\text{calcite/aragonite}}{CaCO_3} + 2H_4SiO_4 + 8H^+$$

$$\underset{\text{serpentine}}{Mg_3Si_2O_5(OH)_4} + 4H_2O + 5CO_2 + 2Ca^{2+} \rightarrow \underset{\text{dolomite}}{2CaMg(CO_3)_2} + \underset{\text{magnesite}}{MgCO_3} + 2H_4SiO_4 + 4H^+$$

$$3\underset{\text{serpentine}}{Mg_3Si_2O_5(OH)_4} + 6H_4SiO_4 + H_2O + 6CO_2 + 3Ca^{2+} \rightarrow \underset{\text{dolomite}}{3CaMg(CO_3)_2} + \underset{\text{sepiolite}}{Mg_8Si_{12}O_{30}(OH)_4(OH_2)_4.8H_2O} + 8H^+$$

$$6\underset{\text{serpentine}}{Mg_3Si_2O_5(OH)_4} + 12H_2O + 20CO_2 + 10Ca^{2+} \rightarrow \underset{\text{dolomite}}{10CaMg(CO_3)_2} + \underset{\text{sepiolite}}{Mg_8Si_{12}O_{30}(OH)_4(OH_2)_4.8H_2O} + 20H^+$$

Textural relations, as captured in SEM images, also show that sepiolite could be derived from dolomite, as formulated below:

$$8\underset{\text{dolomite}}{CaMg(CO_3)_2} + 12H_4SiO_4 \rightarrow \underset{\text{sepiolite}}{Mg_8Si_{12}O_{30}(OH)_4(OH_2)_4.8H_2O} + 16CO_2 + 2H_2O + 16OH^- + 8Ca^{2+}$$

As can be seen clearly from these reactions, the first minerals derived from serpentines were carbonates and silicic acid derived from this reaction was used in the formation of sepiolite, instead of talc and quartz. In other words, the type of neoformed minerals appears to be controlled by the activities of Mg^{2+}/H^+ and H_4SiO_4 (Coleman and Jove, 1992; Birsoy, 2002), and indirectly by pH, which ranges from 7.6 to 8.3 for the sepiolite and dolomite assemblage according to the activity diagram proposed by Birsoy (2002).

In addition, sepiolite, not serpentine, is able to form from olivine in a weathering environment with high pH (Peters, 1993); but textural and mineralogical relations that might confirm the following reaction are not observed in the Elmadağ sepiolites:

$$\underset{\text{forsterite}}{4Mg_2SiO_4} + 8H_4SiO_4 \rightarrow \underset{\text{sepiolite}}{Mg_8Si_{12}O_{30}(OH)_4(OH_2)_4.8H_2O} + 2H_2O$$

Moreover, it is not possible that chlorite and smectite associated in the Elmadağ ophicarbonates formed from serpentine:

$$6\underset{\text{serpentine}}{Mg_3Si_2O_5(OH)_4} + 6H_4SiO_4 + xCa^{2+} \rightarrow \underset{\text{Mg-chlorite}}{Mg_{12}Si_8O_{20}(OH)_{16}} + \underset{\text{Mg-smectite}}{Ca_xMg_6Si_8O_{20}(OH)_4.4H_2O} + 6H_2O + 8OH^-$$

CONCLUSIONS

A new vein type of bedded sepiolite occurrence has been discovered within a 2 m thick, brecciated alteration zone at the contact of tectonites and cumulates of the Elmadağ ophiolitic series. Sepiolites in the ophicarbonates are associated mainly with dolomite, and to a very small extent with serpentine, smectite and chlorite. Fibrous sepiolites occur in voids within dolomitic rocks and at the edges and surfaces surrounding sparitic dolomite. The Elmadağ chain-structure phyllosilicate is termed Al-sepiolite, which is poorer in Mg and Fe, and in some trace elements such as Cr and Ni, than those in the literature.

The mineral assemblages of the Elmadağ ultramafic rocks and ophicarbonates indicate that alteration processes such as serpentinization, uralitization and sepiolitization occurred at different temperatures and times under low-pressure conditions. Epigenetic sepiolite formed by means of dissolution of serpentine by carbon dioxide or carbonic acid-bearing meteoric and/or groundwaters which moved along thrust and shear planes during or after mélange formation. The occurrences of various ophicarbonate associations such as sepiolite and dolomite in the majority, and less significantly calcite, aragonite and magnesite, are related to $Mg^{2+}/(Mg^{2+}+Ca^{2+})$, H_2O/CO_2 and MgO/SiO_2 ratios controlled by the activities of Mg^{2+}/H^+ and H_4SiO_4 and, indirectly, by the pH of the environment.

ACKNOWLEDGMENTS

We thank Nizamettin Akın of Elmadağ Tülü Madencilik for logistical help, chemical engineer Fatma Yalçın and chemist Dr Ümit Şengül for laboratory assistance, and Prof. Dr Işık Ece (Istanbul Technical University) for providing SEM images. The authors are grateful to two anonymous reviewers for their suggestions which led to improvement of the manuscript. We would also like to thank Associate Editor Warren D. Huff (University of Cincinnatti) and Editor-in-Chief, Derek C. Bain (Macaulay Institute, UK) for their constructive comments which encouraged us to revise our manuscript.

REFERENCES

Abu-Jaber, N.S. and Kimberley, M.M. (1992) Origin of ultramafic-hosted vein magnesite deposits. *Ore Geology Reviews*, **7**, 155–191.

Bailey, E.B. and McCallien, W.J. (1950) The Ankara Mélange and the Anatolian Thrust. *Nature*, **166**, 938, 940.

Bailey, S.W. (1988) X-ray diffraction identification of the polytypes of mica, serpentine, and chlorite. *Clays and Clay Minerals*, **36**, 193–213.

Birsoy, R. (2002) Formation of sepiolite-palygorskite and related minerals from solution. *Clays and Clay Minerals*, **50**, 736–745.

Bonatti, E., Emiliani, C., Ferrara, G., Honnorez, J. and Rydell, H. (1974) Ultramafic carbonate breccias from the equatorial Mid-Atlantic Ridge. *Marine Geology*, **16**, 83–102.

Brindley, G.W. (1980) Quantitative X-ray mineral analysis of clays: Pp. 411–438 in: *Crystal Structures of Clay Minerals and their X-ray Identification* (G.W. Brindley and G. Brown, editors). Monograph **5**, Mineralogical Society, London.

Coleman, R.G. (1977) *Ophiolites: Ancient Oceanic Lithosphere*. Springer-Verlag, Berlin, 229 pp.

Coleman, R.G. and Jove, C. (1992) Geological origin of serpentinites. Pp. 1–17 in: *The Vegetation of Ultramafic (Serpentine) Soils*. Proceedings of the First International Conference on Serpentine Ecology (A.J.M. Baker, J. Proctor and R.D. Revees, editors). Intercept Ltd., Andover, United Kingdom.

Çapan, U., Lauer, J.P. and Whitechurch, H. (1983) The Ankara Melange (Central Anatolia): An important element for the reconstruction of Tethyan closure. *Bulletin of Earth Sciences Application and Research Centre of Hacettepe University of Ankara*, **10**, 35–43 (in Turkish, with English abstract).

Çelik, M. (1989) Ankara doğu kesiminin mineralojik – petrografik ve jeokimyasal özelliklerinin incelenmesi. PhD, Hacettepe University Institute of Sciences, Turkey, 256 pp. (unpublished).

Ece, Ö.I. (1998) Diagenetic transformation of magnesite pebbles and cobbles to sepiolite (Meerschaum) in the Miocene Eskişehir lacustrine basin, Turkey. *Clays and Clay Minerals*, **46**, 436–445.

Ece, Ö.I. and Çoban, F. (1994) Geology, occurrence, and genesis of Eskişehir sepiolite, Turkey. *Clays and Clay Minerals*, **42**, 81–92.

Evans, B.W. and Guggenheim, S. (1988) Talc, pyrophyllite, and related minerals. Pp. 225–294 in: *Hydrous Phyllosilicates (Exlusive of Micas)* (S.W. Bailey, editor). Reviews in Mineralogy, **19**. Mineralogical Society of America, Washington, D.C.

Flanagan, F.J. (1976) Descriptions and analyses of eight new USGS rock standards. *Twenty-eight papers present analytical data on new and previously described whole rock standards* (F.J. Flanagan, editor). United States Geological Survey, Professional Paper, **840**, 171–172.

Frost, R.L. and Ding, Z. (2003) Controlled rate thermal analysis and differential scanning calorimetry of sepiolites and palygorskites. *Thermochimica Acta*, **397**, 119–128.

Galán, E. and Carretero, M.I. (1999) A new approach to compositional limits for sepiolite and palygorskite. *Clays and Clay Minerals*, **47**, 399–409.

Govindaraju, K. (1989) 1989 compilation of working values and sample description for 272 geostandards. *Geostandards Newsletter*, **13**, 1–113.

Jones, B.F. and Galán, E. (1988) Palygorskite-Sepiolite. Pp. 631–674 in: *Hydrous Phyllosilicates (Exlusive of Micas)* (S.W. Bailey, editor). Reviews in Mineralogy, **19**. Mineralogical Society of America, Washington, D.C.

Lambert, S.J. and Epstein, S. (1992) Stable-isotope studies of rocks and secondary minerals in a vapor-dominated hydrothermal system at The Geysers, Sonoma County, California. *Journal of Volcanology and Geothermal Research*, **53**, 199–226.

Mittwede, S.K. (1996) Serpentinite-related mineralization. Pp. 144–148 in: *Serpentinites: Records of Tectonic and Petrological History* (D.S. O'Hanley, editor). Oxford Monographs on Geology and Geophysics, **34**. Oxford University Press, Oxford, New York.

Moore, D.M. and Reynolds, R.C., Jr. (1997) *X-ray Diffraction and the Identification and Analysis of Clay Minerals*. Oxford University Press, Oxford, UK, 378 pp.

O'Hanley, D.S. (1996) *Serpentinites: Records of Tectonic and Petrological History*. Oxford Monographs on Geology and Geophysics, **34**. Oxford University Press, Oxford, New York, 277 pp.

Peabody, C.E. and Einaudi, M.T. (1992) Origin of petroleum and mercury in the Culver-Baer cinnabar deposit, Mayacmas district, California. *Economic Geology*, **87**, 1078–1103.

Peters, E.K. (1993) D-^{18}O enriched waters of the Coast Range mountains, northern California: connate and ore-forming fluids. *Geochimica et Cosmochimica Acta*, **57**, 1093–1104.

Sakai, R., Kusakabe, M., Noto, M. and Ishii, T. (1991) Origin of waters responsible for serpentinization of the Izu-Ogawawara-Mariana forearc seamounts in view of hydrogene and oxygen isotope ratios. *Earth and Planetary Science Letters*, **100**, 291–303.

Schandl, E.S. and Wicks, F.J. (1993) Carbonates and associated alteration of ultramafic and rhyolitic rocks at the Hemingwat property, Kidd Creek volcanic complex, Timmins, Ontario. *Economic Geology*, **88**, 1615–1635.

Şengör, A.M.C. and Yılmaz, Y. (1981) Tethyan evolution of Turkey: a plate tectonic approach. *Tectonophysics*, **75**, 181–241.

Şengör, A.M.C. (1979) The North Anatolian fault: its age, offset, and tectonic significance: *Journal of the Geological Society, London*, **136**, 268–282.

Singer, A. and Galán, E. (1984) *Palygorskite-Sepiolite: Occurrences, Genesis and Uses*. Developments in Sedimentology, **37**, Elsevier, Amsterdam, 352 pp.

Taylor, S.R. and McLennan, S.M. (1985) *The Continental Crust: Its Composition and Evolution*. Blackwell, Oxford, UK, 312 pp.

Weaver, C.E. and Pollard, L.D. (1973) *The Chemistry of Clay Minerals*. Developments in Sedimentology, **15**, Elsevier, Amsterdam, 213 pp.

Wicks, F.J. and O'Hanley, D.S. (1988) Serpentine minerals: structures and petrology. Pp. 91–167 in: *Hydrous Phyllosilicates (Exlusive of Micas)* (S.W. Bailey, editor). Reviews in Mineralogy, **19**. Mineralogical Society of America, Washington, D.C.

Wicks, F.J. and Plant, G. (1979) Electron microprobe and X-ray microbeam studies of serpentine textures. *The Canadian Mineralogist*, **17**, 785–830.

Wicks, F.J. and Whittaker, E.J.W. (1977) Serpentine textures and serpentinization. *The Canadian Mineralogist*, **15**, 459–488.

Yalçın, H. and Bozkaya, Ö. (1995a) Mineralogy and geochemistry of lacustrine palygorskites from Kangal-Çetinkaya subbasin (Sivas basin), Central Eastern Anatolia, Turkey. *Proceedings of VIIth Turkish National Clay Symposium* (M. Şener, F. Öner and E. Koşun, editors). MTA, Ankara, pp. 105–116 (in Turkish, with English abstract).

Yalçın, H. and Bozkaya, Ö. (1995b) Sepiolite-palygorskite from the Hekimhan region (Turkey). *Clays and Clay Minerals*, **43**, 705–717.

Yeniyol, M. (1986) Vein-like sepiolite occurrence as a replacement of magnesite in Konya, Turkey. *Clays and Clay Minerals*, **34**, 353–356.

Yeniyol, M. (1992) Yenidoğan (Sivrihisar) sepiolit yatağının jeolojisi, mineralojisi ve oluşumu. *Maden Tetkik ve Arama Dergisi*, **114**, 71–84 (in Turkish).

Yeniyol, M. (1993) Sivrihisar'da (Eskişehir) sedimanter-diyajenetik oluşÞumlu yeni bir lületaşı türü. *Maden Tetkik ve Arama Dergisi*, **115**, 81–90 (in Turkish).

Yılmaz, Y., Tüysüz, O., Yiğitbaş, E., Genç, Ş.C. and Şengör, A.M.C. (1997) Geology and tectonic evolution of the Pontides. Pp. 183–226 in: *Regional and Petroleum Geology of the Black Sea and Surrounding Region* (A.G. Robinson, editor). American Association of Petroleum Geologists Memoir, **68**, Tulsa, Oklahoma.

(*Received 29 January 2003; revised 14 October 2003; Ms. 757; A.E. Warren D. Huff*)